

Erratum

The potential value of cuprotosis (copper-induced cell death) in the therapy of clear cell renal cell carcinoma: Am J Cancer Res. 2022; 12(8): 3947-3966

Xiaochen Qi, Jin Wang, Xiangyu Che, Quanlin Li, Xiaowei Li, Qifei Wang, Guangzhen Wu

Department of Urology, The First Affiliated Hospital of Dalian Medical University, Dalian 116011, Liaoning, China

Received March 23, 2024; Accepted April 9, 2024; Epub May 15, 2024; Published May 30, 2024

In this article, we found that our two figures (**Figures 1** and **4**) have errors in the order of layer coverage. So, we would like to publish this erratum to reflect this change. We apologize for the wrong figures we provided.

The corrected **Figures 1** and **4** are as follows.

Address correspondence to: Guangzhen Wu and Qifei Wang, Department of Urology, The First Affiliated Hospital of Dalian Medical University, No. 222 Zhongshan Road, Dalian 116011, Liaoning, China. Tel: +86-18098876012; E-mail: wuguangzhen@firsthosp-dmu.com (GZW); Tel: +86-1809887-6008; E-mail: wangqifei6008@hotmail.com (QFW)

Cuproptosis in ccRCC targeted therapy

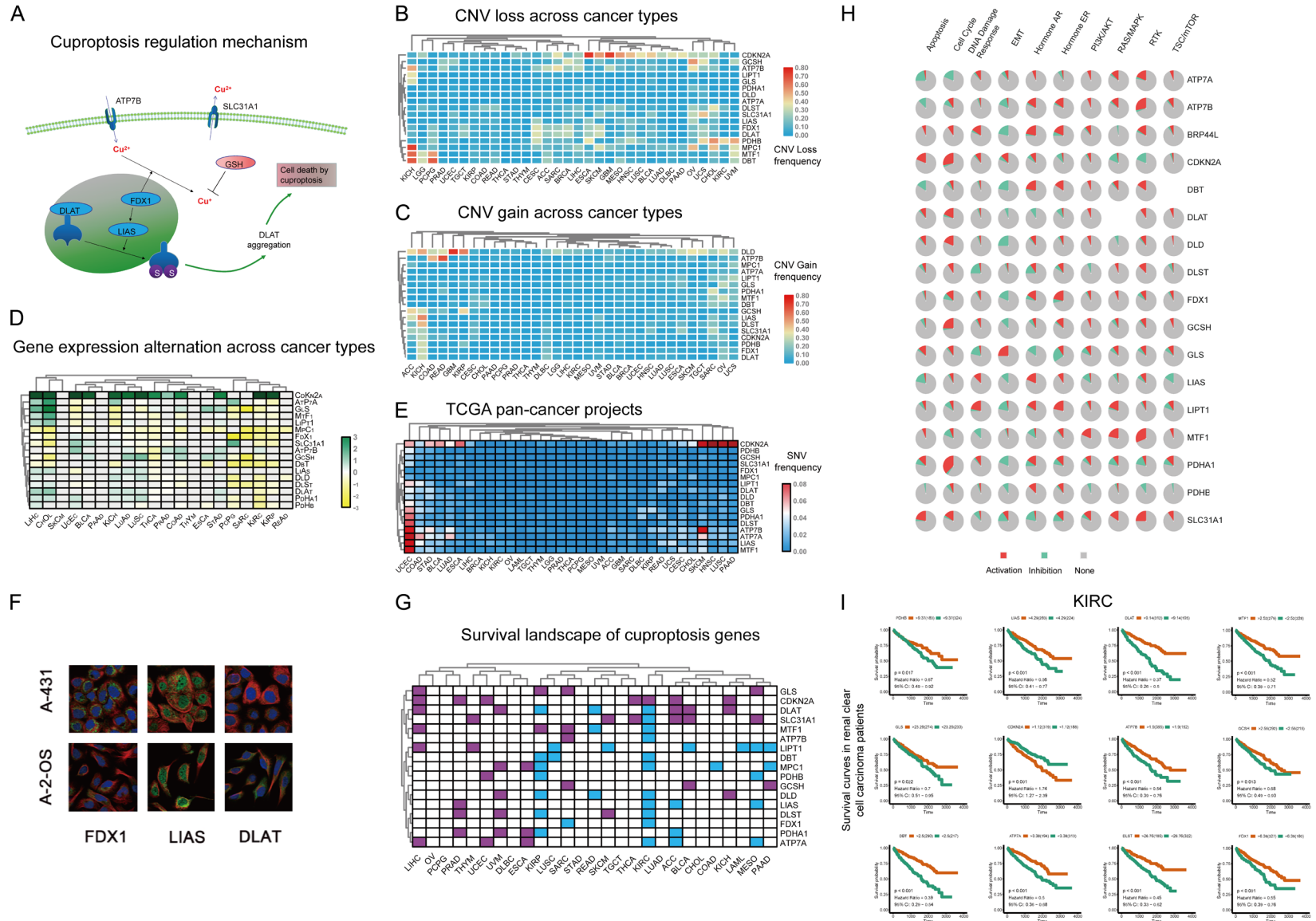
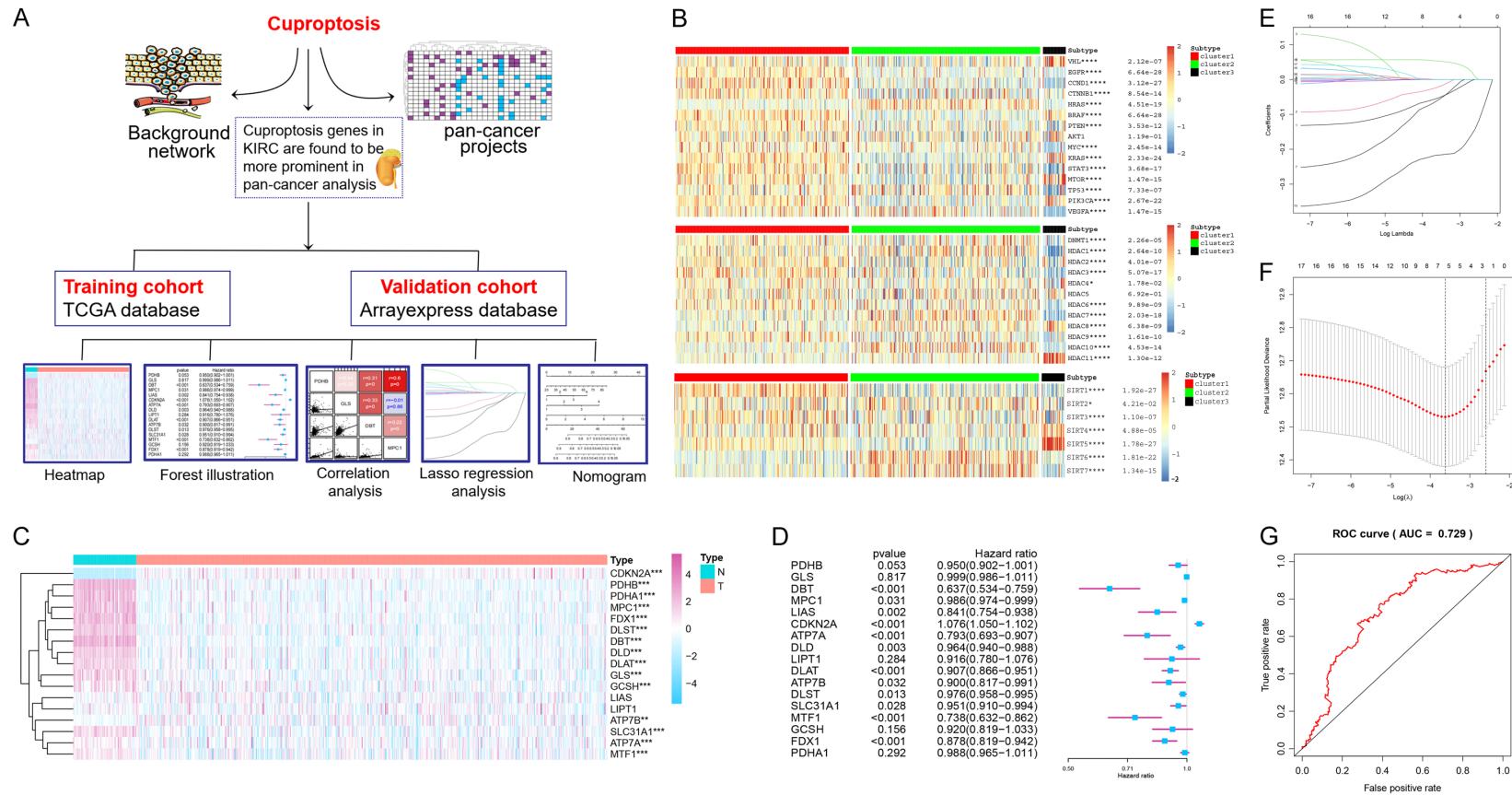


Figure 1. Pan-cancer analysis and molecular mechanism. A. The mechanism of cell death caused by cuproptosis. The massive accumulation of DLAT bound to sulfur atoms is the direct cause of cuproptosis. B, C. CNV (copy number variation) representation of Cuproptosis-related genes in 33 cancers. B, C. Represent CNV gain and

Cuproptosis in ccRCC targeted therapy

CNV loss, respectively. The color bar on the right represents the CNV gain/loss frequency, from blue to red corresponding to the degree from low to high. D. The heat map shows the expression of cuproptosis-related genes in 33 cancers after taking the logarithm of the ratio of expression levels in cancer and normal tissues. The color bar on the right indicates that the color from yellow to green corresponds to the ratio of expression levels from low to high. E. SNV (single nucleotide variation) representation of Cuproptosis-related genes in 33 cancers. The color bar on the right represents the SNV frequency, from blue to red corresponding to the degree from low to high. F. Immunofluorescence showed the expression distribution of the proteins corresponding to the three key genes (FDX1, LIAS, DLAT) in A-2-OS and A-431 cell lines. G. Combined with the survival information of the samples, the properties of cuproptosis-related genes in 33 cancers were judged, and they were classified as protective genes or risk genes. Among them, blue represents protective genes and purple represents risk genes. H. The roles and weights of cuproptosis-related genes in various classical oncogenic pathways, blue represents activation and red represents inhibition. I. Survival curves of 12 cuproptosis-related genes with statistical significance in ccRCC based on their expression levels and the clinical survival information of the samples.



Cuprotosis in ccRCC targeted therapy

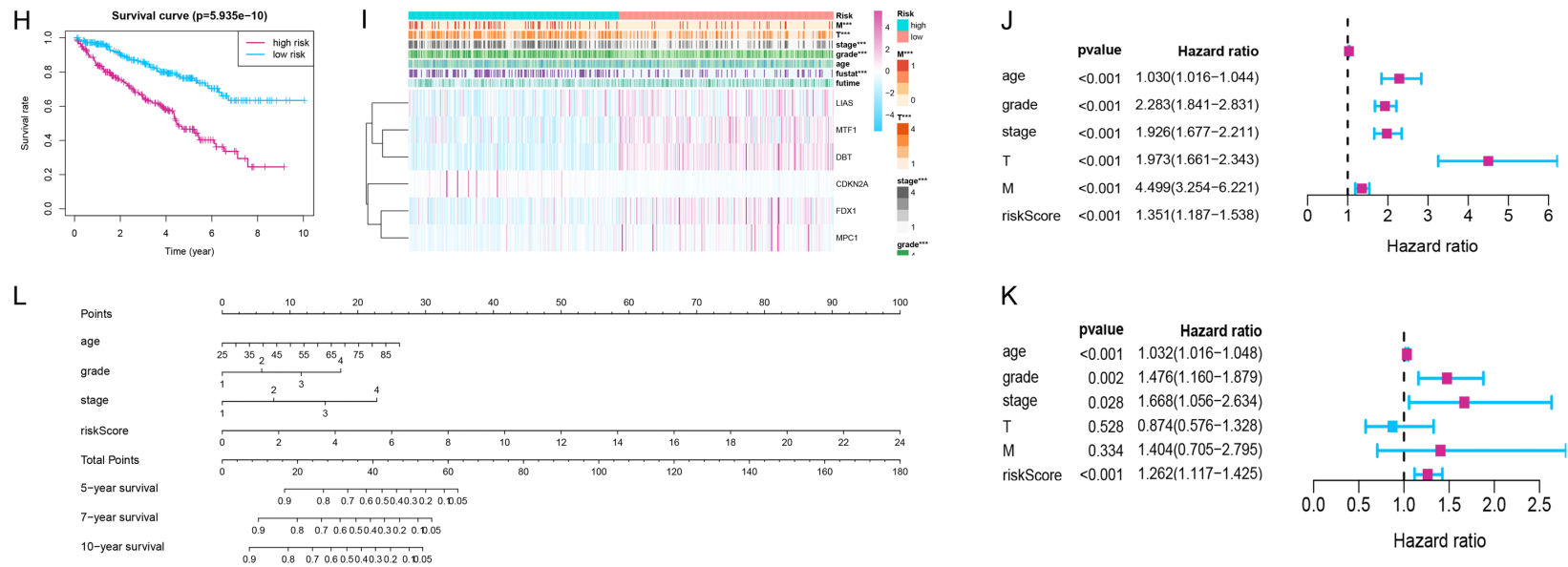


Figure 4. Construction of clinical prognostic model. A. A cuprotosis-related prognostic model of ccRCC patients was constructed by combining the gene expression data in the TCGA cohort samples with the clinical and pathological characteristics data for analysis. B. The heat map shows the gene expression of canonical oncogenes of ccRCC, HDAC family, and SIRT family in the three clustered samples, respectively (*: $p < 0.05$, **: $p < 0.01$, ***: $p < 0.001$, ****: $p < 0.0001$). C. Comparison of the expression of cuprotosis-related genes between cancer tissue cohorts and normal tissue cohorts in the TCGA database. D. The forest plot shows the Hazard ratio value and P value of each cuprotosis-related gene after COX regression analysis. E, F. 6 genes were screened from 17 cuprotosis-related genes by LASSO regression as risk-score features for building survival prediction models. G. ROC curve of the 10-year survival prediction model constructed based on cuprotosis-related genes and features of clinical and pathological. H. Survival curves of high-risk and low-risk groups adjudicated with the median as the cutoff. I. The heat map shows the comparison of the clinical characteristics, pathological characteristics, and expression levels of the six genes screened by LASSO regression between the high-risk group and the low-risk group. J. The Hazard ratio and P value of each feature used to construct the survival prediction model were calculated by univariate COX regression. K. The Hazard ratio and P value of each feature used to construct the survival prediction model were calculated by multivariate COX regression. L. Display the resulting predictive model with a Nomogram.